

Muonic-hydrogen molecular bound states, quasibound states, and resonances in the Born-Oppenheimer approximation

J. David Jackson

Lawrence Berkeley Laboratory and Department of Physics, University of California at Berkeley, Berkeley, California 92720

(Received 14 June 1993)

The Born-Oppenheimer approximation is used as an exploratory tool to study bound states, quasibound states, and scattering resonances in muon (μ)-hydrogen (x)-hydrogen (y) molecular ions. Our purpose is to comment on the existence and nature of the narrow states reported in three-body calculations, for $L=0$ and 1, at approximately 55 eV above threshold and the family of states in the same partial waves reported about 1.9 keV above threshold. We first discuss the motivation for study of excited states beyond the well-known and well-studied bound states. Then we reproduce the energies and other properties of these well-known states to show that, despite the relatively large muon mass, the Born-Oppenheimer approximation gives a good, semiquantitative description containing all the essential physics. Born-Oppenheimer calculations of the s - and p -wave scattering of d -($d\mu$), d -($t\mu$), and t -($t\mu$) are compared with the accurate three-body results, again with general success. The places of disagreement are understood in terms of the differences in location of slightly bound (or unbound) states in the Born-Oppenheimer approximation compared to the accurate three-body calculations. The analytic properties of the function $k^{2L+1}\cot\delta$ are used to illustrate the locating of bound states and resonance poles in the complex k or E plane from the scattering data and to deduce the expected widths of resonances of a given L value. The prominent $L=3$ resonance at 22 eV ($\Gamma=1.4$ eV) in d -($t\mu$) scattering provides a benchmark for the unsuccessful search within the Born-Oppenheimer approximation for the claimed narrow s -wave d - t - μ resonance at 54.35 eV ($\Gamma=0.74$ eV). Although absolute proof is obviously lacking (because of the approximate calculation), the Born-Oppenheimer results for the s -wave *gerade* scattering are entirely reasonable; the absence of a centrifugal barrier makes it implausible that there could be resonances at 50–60 eV with narrow widths. We argue that the threshold at 48 eV of the t + ($d\mu$) channel is unlikely to have a major effect. The family of states at 1.9 keV and above are of a different nature. They are, as is already known, molecular states based on the $3d\sigma_g$ “electronic” potential-energy curve, which is asymptotically the energy of the $x(y\mu; n=2)$ system. Born-Oppenheimer calculations of binding energies, and properties depending dominantly on the wave functions in the classically allowed region, agree reasonably well with the accurate three-body computations for the d - t - μ system. Expected disagreement occurs in the probability density $\rho_N(0)$ for the nuclei to be at vanishing internuclear separation (relevant for the fusion rate), in which configuration mixing is more important in the classically forbidden region. Nonetheless, the reported values of $\rho_N(0)$, when compared to the average probability density in the classically allowed region of nuclear motion computed here, appear excessively large. The likelihood that this family of continuum resonances would play a significant role in molecular formation in the muonic cascade is discussed briefly.

PACS number(s): 36.10.Dr

I. INTRODUCTION

The old subject of the catalysis of nuclear fusion between isotopes of hydrogen by negative muons has experienced a resurgence in the past 15 years because of the discovery of very rapid molecular formation rates ($\lambda > 10^8 \text{ s}^{-1}$ for normal liquid hydrogen density) because of the existence of loosely bound excited states of the molecular ion within less than 2 eV of threshold for the d - d - μ and d - t - μ systems. The original experiments and detailed theoretical calculations of the 1970s were done largely in the former Soviet Union. The history and references are given in the review by Ponomarev [1]. With other processes proceeding at least as rapidly as molecular formation, the cycling rate of the muons can be 100 or more times faster than the natural decay rate.

There would seem to be the prospect of hundreds of catalytic acts per muon, if nothing else interfered. The reality is that something does interfere. In its facilitation of the fusion act, in d - t - μ or d - d - μ , for example, the muon has a finite probability ω_0 of being captured into a bound state around the recoiling helium or hydrogen ion(s) (initial sticking). As the ion slows down to rest, there is a probability R that the muon will be stripped off (reactivation), but the end result is a sticking probability $\omega_s = \omega_0(1 - R)$ for loss of the muon to the cycle. The maximum number of fusions per muon is bounded by $1/\omega_s$. The original estimates [2] for d - t - μ were $\omega_0 \approx 1.2\%$ and $R \approx 0.22$, leading to $\omega_s \approx 1.0\%$. More recent and accurate calculations [3] of ω_0 , not restricted to the Born-Oppenheimer approximation for the muonic molecule, and new evaluations [4,5] of R , including density dependence, give

$\omega_0 = 0.886\%$ and $\omega_s \approx 0.64\%$ at low density and $\omega_s \approx 0.58\%$ at 1.2 times liquid-hydrogen density. The experimental situation is somewhat contradictory, with some experiments showing a relatively small density dependence in agreement with theory, but a magnitude that is 20% smaller than theory, and other experiments seeming to show a more rapid variation with density and values at high densities that are roughly one-half the theoretical result. See Fig. 19 of Ref. [1] or Fig. 3 of Ref. [5].

Despite the uncertainty about the exact value of ω_s , the sticking mechanism is presently the limitation in the prospects of realizing useful energy production from muon-catalyzed fusion alone. There have been many investigations of ways to modify or get around the problem of sticking. These fall into two classes. The first concentrates on the reactivation process, the second on the initial sticking probability. The size of ω_0 is a property of the molecular state before fusion and, in principle, on the temporal details of the nuclear reaction.

The time scales and energies of the molecular dynamics and of the nuclear reaction are so different that the nuclear reaction proceeds as for free nuclei at zero energy, independent of the particular molecular state from which fusion occurs (orbital angular momentum, spin and parity, and the nuclear wave function at short distances are relevant, of course). The muon's motion is different, however, in different molecular states. The following question then arises: Are there molecular states with sufficiently rapid fusion rates, but with smaller initial sticking probabilities? The bound states of the x - y - μ molecular ion (based on the $1s \sigma_g$ potential, in the language of the Born-Oppenheimer approximation) have been studied in great detail in recent years with complete three-body dynamics [6,7]. The properties of the ground and excited bound states with orbital angular momentum $L=0$ and 1 have been reliably calculated and the initial sticking probabilities all determined. The results quoted above are based on these computations. In a search for other molecular states that might enter (or somehow be made to enter) the complex cascade of the muon (from keV energies when liberated in a fusion, through atom formation, scattering, and transfer from a lighter isotope to a heavier one, and finally to thermal or epithermal energies where the atom unites with a nucleus to form the molecular ion), attention has focused on continuum resonances.

A narrow s -wave resonance ($\Gamma=0.74$ eV) at a center-of-mass system (c.m.s.) energy of $E_0=54.35$ eV above the d - $t\mu(1s)$ threshold has been found in elaborate three-body calculations of the d - t - μ system [8,9], with a p -wave resonance nearby ($E_0=54.63$ eV, $\Gamma=2.04$ eV). Families of higher-lying resonances have similarly been calculated [10–12]. These are s - and p -wave resonances located less than 220 eV below the d - $t\mu(2s)$ threshold (which lies 2 keV above the ground-state threshold). This second set of states [which we call $n=2$ states, in contrast to the states near or below the d - $t\mu(1s)$ threshold, which we label $n=1$] has nothing to do with the putative $n=1$ resonance at 54 eV. In Ref. [12] it is argued that the fusion rates from the lowest three of the $n=2$ s -wave states are

comparable to that of the $n=1$ ground state and comparable to the widths (0.0027–0.51 eV) computed ignoring fusion. It is inferred that these states may play a role in epithermal fusion if the molecule formation rates are large enough to compete with the rapid deexcitation of the atomic $t\mu(2s)$ state. Very recently, calculations have been reported of the sticking probabilities ω_0 (and revised energies and widths) for these three states [13]. The values of ω_0 are from five to nine times smaller than for the $n=1$ ground state. It is pointed out that, if these resonances play some role in the fusion process, the smaller values of initial sticking could offer an explanation for the 20% discrepancy between theory and experiment mentioned above.

In Refs. [8], [9], and [11] it is argued that the resonances found above the $n=1$ threshold and below the $n=2$ threshold are “Feshbach resonances,” in analogy to certain resonances built on excited orbitals in nuclear physics [14,15] and cannot appear in the Born-Oppenheimer approximation. In fact, the physical mechanism of the $n=2$ resonances below the d - $t\mu(2s)$ threshold has been explained very adequately [16] in terms of the Born-Oppenheimer approximation, using “electronic” potentials associated with the asymptotic hydrogenic state with $n=2$ [denoted $3d \sigma_g$ ($3 \sigma_g$) and $2s \sigma_g$ ($2 \sigma_g$) for the lowest gerade states, for example]. We argue here that the three-body system of muon and two hydrogen nuclei, with only one light particle, is so simple that the language of Feshbach resonances is inappropriate, particularly for states lying far below the nearest excited orbital energy. Terminology apart, we show that the Born-Oppenheimer approximation, while not of sufficient quantitative precision for all purposes, gives not just a qualitative but a semiquantitative understanding of the properties of the bound and continuum states. By establishing its ability to describe correctly the physics, if not the precise numbers, we justify the use of the Born-Oppenheimer approximation as a tool to comment on the properties found for the continuum states by the large-scale numerical computations. We make no apology for treading in the footsteps of Gershtein, who studied the x - y - μ bound states in the Born-Oppenheimer approximation in his Ph.D. thesis in 1958. Simple tools can often bring physics to the fore better than huge numerical computations.

In order to verify its semiquantitative validity and see its limitations, we first present results of the simplest Born-Oppenheimer approximation for the ($n=1$) x - y - μ bound states, with $(x,y)=(p,p)$, (p,d) , (p,t) , (d,d) , (d,t) , and (t,t) . Binding energies, nuclear densities at zero separation of the nuclei for $L=0$ states, and the corresponding quantities for $L=1$ states are compared with the more precise results [6,7,17–19].

The low-energy scattering is then discussed for the d - $d\mu(1s)$, d - $t\mu(1s)$, and t - $t\mu(1s)$ systems in the partial waves, $L=0$ and 1. Comparisons are made with the accurate computations [20,21]. The $L=0$ cross sections compare very favorably, but the $L=1$ do not. For d - $d\mu(1s)$, the disagreement is caused by the fact that the (1,1) state in the Born-Oppenheimer calculation does not appear as a bound state at -1.975 eV, but as a resonance

with a width of about 2–3 eV at around 2 eV. For $d-t\mu(1s)$, the discrepancy is caused by the presence in the precise three-body calculations of the (1,1) bound state at -0.660 eV just below threshold, while in the Born-Oppenheimer approximation the bound state is at -7.7 eV. The issue of resonances and nearby bound states leads naturally to an exploitation of the analytic properties of $k^{2L+1}\cot\delta$ to determine the locations of resonance poles and bound states in the complex k or E plane. Polynomial fits in k^2 to $k^{2L+1}\cot\delta$ over finite energy ranges are made for the $L=1$ scattering of $d-d\mu(1s)$ and $d-t\mu(1s)$ to show the power and limitations of the technique in the location of resonant poles and bound states.

The $L=3$ partial wave of the low-energy $d-t\mu(1s)$ system is of particular interest. The centrifugal barrier is high enough to cause a relatively narrow resonance to appear at 22 eV with a width of 1.4 eV, as can be inferred from the precise three-body computations of Chiccoli *et al.* [21]. In the Born-Oppenheimer approximation, the same resonance, characterized as a quasistable (3,0) state, is expected from the shape of the effective potential-energy curve and appears (at 16 or 17 eV and a width of 1.2 eV). This state provides more evidence that the Born-Oppenheimer approximation misses little, if any, of the physics.

The $L=0$ $d-t\mu(1s)$ scattering phase for the gerade state is examined for evidence of a narrow resonance at 54 eV. There is no evidence for such a state; the phase shift falls smoothly with energy from its value of 2π at zero, reaching π at about 100 eV. Needless to say, a search for resonant poles using polynomial fits in k^2 to $k\cot\delta$ yields no narrow resonance either.

The energies and other properties of the $n=2$ resonant states are calculated and compared with the three-body calculations of Refs. [10–13]. In the Born-Oppenheimer approximation, these states are quasibound states in the potential formed from the Coulomb repulsion of the nuclei and the energy of the lowest excited electronic state, which asymptotically goes over to a bare nucleus and a neutral hydrogenlike atom in the $n=2$ state. As already demonstrated by Shimamura [16], the states in Ref. [10–13] are basically the same as found via the Born-Oppenheimer approximation. Some peculiarities of the results of Refs. [12] and [13] for the fusion rates, or equivalently the nuclear densities at zero nuclear separation, are pointed out.

The nonrelativistic electronic energies of a negatively charged point particle in the presence of two equal, fixed, positive point charges is exactly soluble in terms of “known” functions. Numerical tables for a large number of electronic states exist [22,23] and accurate computations for some states have been made in the course of three-body computations [24]. The discrete array of tabulated values for the states of interest were interpolated approximately by explicit functional forms so that the Schrödinger equation for the nuclear motion could be solved straightforwardly. The representations for the potential energy curves needed here are collected in the Appendix. There are no claims of uniqueness or optimization; the fits are adequate for my purposes. Unless otherwise stated, atomic (hartree) units are used, with energies

in units of $e^2/a_\mu = 5626.48$ eV and lengths in units of $a_\mu = 2.55927 \times 10^{-11}$ cm.

For the nuclear relative motion, exact nuclear masses are used to determine the reduced masses. In the spirit of the Born-Oppenheimer approximation, these reduced masses do not include any part of the muon mass. In the discussion of scattering, however, the proper kinematics [of d scattered by $t\mu(1s)$, for example] are used to connect the energy and wave number scales. The relevant potential-energy curves for the $n=1$ and 2 sets of states are shown in Fig. 1. For the excited band, only the lowest gerade potentials $2s\sigma_g$ and $3d\sigma_g$ are shown.

II. $n=1$ BOUND STATES

The Schrödinger equation for the radial relative motion was integrated using the potential energy

$$V(x) = \frac{1}{x} + E_\mu(1s\sigma_g|x) + \frac{L(L+1)\mu}{2Mx^2}, \quad (1)$$

where μ is the muon mass and M is the reduced mass of the nuclei, and E_μ is taken from the Appendix. All the bound-state energies were determined for $L=0$ and 1 for the systems $x-y-\mu$, with $(x,y) = (p,p), (p,d), (p,t), (d,d), (d,t)$, and (t,t) . The results are shown in Fig. 2 as a function of the ratio μ/M , together with the precise three-body results of Refs. [6] and [7]. Both sets of values show a gross tendency for decreasing binding energies with increasing μ/M . The smooth decrease for the Born-Oppenheimer energies can be thought of as a result of the frequency of small oscillations about the equilibrium separation varying as $(\mu/M)^{1/2}$. For the molecules

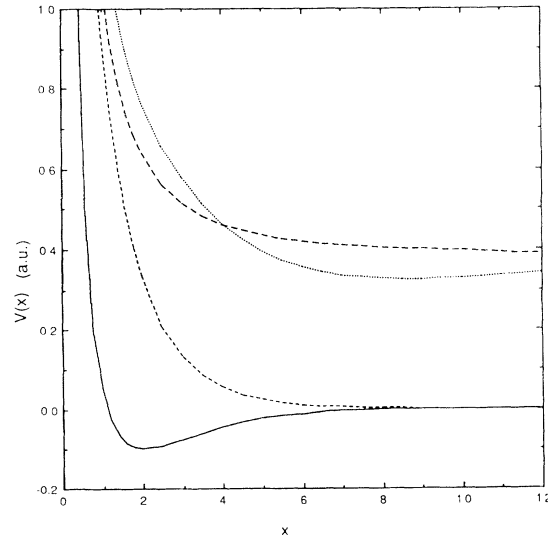


FIG. 1. Born-Oppenheimer molecular potential-energy curves for $x-y-\mu$ ions in muonic hartree units (5626.48 eV for muons) as functions of radial distance in units of a_μ . Solid curve, $1s\sigma_g$; short-dashed curve, $3p\sigma_u$ (sometimes denoted $2p\sigma_u$ or $1\sigma_u$); dotted curve, $3d\sigma_g$; long-dashed curve, $2s\sigma_g$. The zero of energy is the energy of a separated nucleus x and a $y-\mu$ atom in its $1s$ ground state. The upper pair of curves approach the difference in energy of the atom in its $2s$ and $1s$ states. Only two of the several $n=2$ potential-energy curves are shown.

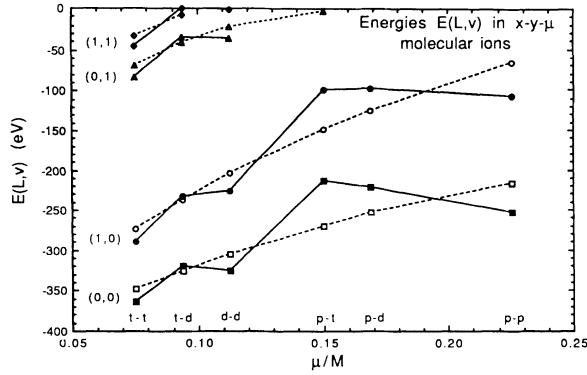


FIG. 2. Comparison of the $L=0$ and 1 energies of $x-y-\mu$ bound states in the Born-Oppenheimer approximation and accurate three-body calculations (Refs. [6] and [7]), displayed as a function of μ/M .

not containing a proton, the Born-Oppenheimer energies are with 10 or 20 eV of the exact energies for all the bound states. For the molecules containing a proton ($\mu/M \geq 0.15$), the differences are as great as 56 eV. With one nuclide fixed, there is a trend with decreasing mass of the other nuclide that goes counter to the trend with increasing μ/M . Some of this trend can be attributed to the reduced mass effect on the binding of the isolated (heavier) atom, relative to which the molecular binding energy is measured. For example, the muon is 183 eV less tightly bound around a proton than a triton; the accurate binding energy for the (0,0) state of the $p-p-\mu$ is 39 eV greater than that for the $p-t-\mu$ system, while the Born-Oppenheimer energies differ by 54 eV in the opposite direction, a total difference of 93 eV in the expected direction.

For the (1,1) states, which have relatively small binding energies, errors of the order of 10 eV mean that the Born-Oppenheimer calculations may not be even qualitatively correct, at least in the counting of the number of bound states. For example, in the $d-t-\mu$ system the Born-

Oppenheimer energy is -7.8 eV for the (1,1) state, to be compared with -0.660 eV from Ref. [6]. For $d-d-\mu$, the bound (1,1) state (at -1.975 eV according to Ref. [6]) is not found in the Born-Oppenheimer calculations. In the $t-t-\mu$ molecule, the (1,1) state energy is -33 eV (Born-Oppenheimer) versus -45.210 eV (Ref. [6]). As we show in Sec. III, the Born-Oppenheimer version of the (1,1) state in the $d-d-\mu$ molecule is not far away, appearing as a scattering resonance a few volts about threshold.

In Fig. 3 we show a comparison of the Born-Oppenheimer nuclear probability densities at zero internuclear separation $\rho_{BO}(0)$ with the precise calculations of Refs. [17–19] for the (0,0) ground state in the various $x-y-\mu$ molecules. The quantitative agreement is satisfactory for all the molecules, poorest for the $p-p-\mu$ system as expected, but even there the discrepancy is less than 30%. (Some factors of 4π have been corrected in the results of Refs. [18] and [19] for this comparison.) We note particularly this and other properties of the (0,0) ground state in the $d-t-\mu$ molecule:

$$\langle r \rangle = 2.7a_\mu, \quad \rho(0) = 0.6 \times 10^{26} \text{ cm}^{-3},$$

$$\langle |\psi(x)|^2 \rangle_{CTP} \approx 2200 \times 10^{26} \text{ cm}^{-3}.$$

Here $\langle r \rangle$ is the mean nuclear separation and $\langle |\psi(x)|^2 \rangle_{CTP}$ is the average value of the square of the Born-Oppenheimer wave function of relative nuclear motion between the classical turning points. (The corresponding quantity in the three-body calculations is called the square of the pseudo-wave-function; it is the integral of the square of the three-body wave function over the muon's coordinates with the internuclear separation held fixed. Between the classical turning points, the precise pseudo-wave-function squared and the Born-Oppenheimer approximation agree reasonably well.) We note a factor of roughly 3600 decrease in probability density from $x \approx 2-3$ to $x=0$, a result of the presence of the Coulomb barrier.

Figure 4 shows a comparison for the lowest $L=1$ state, (1,0), of the square of the gradient of the Born-Oppenheimer wave function at zero internuclear separa-

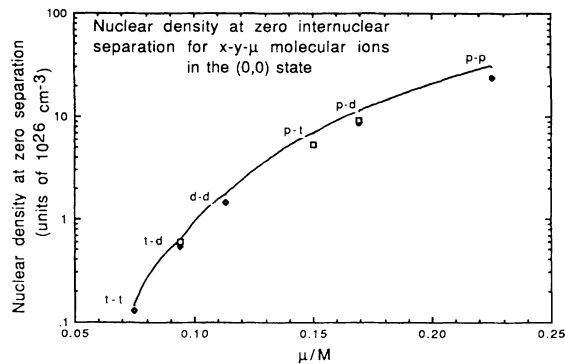


FIG. 3. Comparison of the nuclear densities at zero internuclear separation in units of 10^{26} cm^{-3} for $x-y-\mu$ molecules in the $n=1$ (0,0) state, calculated in the Born-Oppenheimer approximation and in three-body calculations. The Born-Oppenheimer results are given by the curve. The solid diamonds are from Ref. [17]; the open squares are from Refs. [18] and [19].

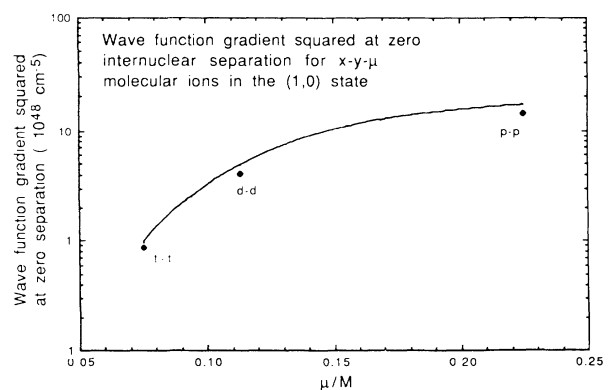


FIG. 4. Comparison of the squares of the gradient of the Born-Oppenheimer wave function at zero internuclear separation (solid curve) with the equivalent three-body quantities from Ref. [17]. Units are 10^{48} cm^{-5} .

tion with the corresponding quantity from the precise three-body calculations of Ref. [17]. Again the agreement is satisfactory.

The excited ($n=2$) "bound" states are discussed in Sec. VI.

III. SCATTERING

The scattering in $L=0$ and 1 partial waves is calculated in the Born-Oppenheimer approximation by integrating the Schrödinger equation for c.m.s. energy E (relative to the appropriate threshold) with the potential (1) for the gerade (symmetric state) and the corresponding ungerade potential, using $E_\mu(2p \sigma_u | x)$ from the Appendix for the antisymmetric state. The radial equation is integrated out to $x=20$ or 30, where the logarithmic derivative is matched to the appropriate combination of r times spherical Bessel functions of argument kr to determine the phase shift. This procedure means that we are truncating the asymptotic potential $-9/4x^4$ at $x=20$ or 30. Negligible error is introduced in the phase shifts by the truncation. In order to take into account properly the kinematics of the asymptotic scattering state, the following (slightly inconsistent) procedure is adopted. In the integration of the Schrödinger equation, the muon's mass is ignored in determining the reduced mass for the relative motion, just as for the bound states. The gerade and ungerade eigenstates are thus treated as degenerate; differences between open and closed channels are ignored. However, in relating the energy E to the square of the wave number k , we treat the nonrelativistic kinematics correctly, that is, the reduced mass M_{red} in the relation $E = k^2 \mu / 2M_{\text{red}}$ is $M_{\text{red}} = m_A(m_B + \mu) / (m_A + m_B + \mu)$, where the asymptotic state is $A + (B\mu)$. Spin is ignored in the dynamics, but is taken into account in handling the symmetry properties for identical nuclei.

For scattering with nonidentical nuclei, there is elastic scattering and charge-exchange scattering, i.e., $A + (B\mu) \rightarrow A + (B\mu)$ and $A + (B\mu) \rightarrow (A\mu) + B$. The c.m.s. elastic scattering and the charge-exchange amplitudes are [25]

$$f_{\text{el}} = \frac{1}{2}(f_g + f_u), \quad f_{\text{cex}} = \frac{1}{2}(f_g - f_u), \quad (2)$$

where f_g (f_u) are the c.m.s. scattering amplitudes for the gerade (ungerade) electronic plus nuclear potentials. In our approximation, the scattering and charge exchange cross sections are

$$\frac{d\sigma}{d\Omega_{\text{el}}} = \frac{1}{4}|f_g + f_u|^2, \quad \frac{d\sigma}{d\Omega_{\text{cex}}} = \frac{k_f}{4k_i}|f_g - f_u|^2. \quad (3)$$

Here k_i and k_f are the wave numbers in the initial and final states and are the only bearers of information about the different thresholds. The cross sections for individual partial waves involve the phase shifts $\delta_g(L)$ and $\delta_u(L)$ in the obvious way.

For identical nuclei, the symmetry or antisymmetry of the various states must be taken into account. For identical spin- $\frac{1}{2}$ nuclei (p - p and t - t), the Pauli principle requires singlet spin states to scatter via the gerade potential for even L and the ungerade potential for odd L . For the

triplet states, it is the reverse. The nuclear-spin-averaged elastic cross section for spin- $\frac{1}{2}$ identical nuclei can be written as [26]

$$\begin{aligned} \frac{d\sigma}{d\Omega_{\text{el}}} &= \frac{1}{16}|f_g(\theta) + f_g(\pi - \theta) + f_u(\theta) - f_u(\pi - \theta)|^2 \\ &+ \frac{3}{16}|f_u(\theta) + f_u(\pi - \theta) + f_g(\theta) - f_g(\pi - \theta)|^2. \end{aligned} \quad (4)$$

The total-elastic-scattering cross section is obtained by integration over all of 4π (in contrast to identical particle scattering) because the atom ($A\mu$) is distinguishable from the nucleus A . The $L=0$ and 1 partial wave cross sections are therefore

$$\begin{aligned} \sigma_0 &= \pi(|A_{g0}|^2 + 3|A_{u0}|^2), \\ \sigma_1 &= 3\pi(|A_{u1}|^2 + 3|A_{g1}|^2). \end{aligned} \quad (5)$$

Here the amplitudes A_{gL} and A_{uL} are the standard amplitudes $e^{i\delta} \sin \delta / k$ for the designated potential and partial waves.

For identical spin-1 nuclei, the spin $S=0, 2$ states are symmetric in spin exchange while the $S=1$ state is antisymmetric. For the $S=0, 2$ states (total weight $\frac{2}{3}$ in the spin-averaged cross section), the scattering in L even (odd) states is via the gerade (ungerade) potential. For $S=1$ (spin weight $\frac{1}{3}$) it is the reverse. The differential cross section has the same form as Eq. (4), but with the factor of $\frac{1}{16}$ replaced by $\frac{1}{6}$ and the factor of $\frac{3}{16}$ replaced by $\frac{1}{12}$. The nuclear-spin-averaged total partial wave cross sections for $L=0$ and 1 are

$$\begin{aligned} \sigma_0 &= \frac{4\pi}{3}(2|A_{g0}|^2 + |A_{u0}|^2), \\ \sigma_1 &= 4\pi(2|A_{u1}|^2 + |A_{g1}|^2). \end{aligned} \quad (6)$$

Figures 5–7 illustrate the Born-Oppenheimer $L=0$ cross sections for $d + (d\mu)$, $d + (t\mu)$, and $t + (t\mu)$ elastic scattering on the energy range from threshold to 100 eV.

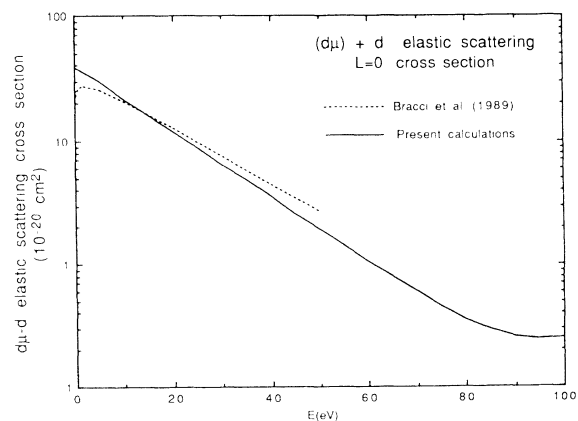


FIG. 5. Comparison of spin-averaged $L=0$ elastic scattering cross section for $d + (d\mu)$ in the Born-Oppenheimer approximation with accurate three-body results. Solid curve, present calculations; dotted curve, Ref. [20].

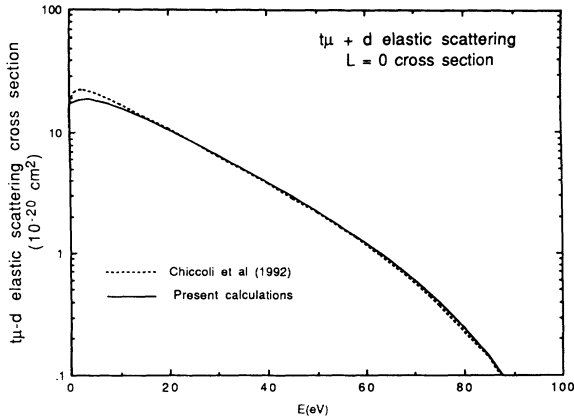


FIG. 6. Comparison of spin-averaged $L=0$ elastic scattering cross section for $d+(t\mu)$ in the Born-Oppenheimer approximation with accurate three-body results. Solid curve, present calculations; dotted curve, Ref. [21].

The comparison curves are from Ref. [20] for $d+(d\mu)$ and $t+(t\mu)$ and Ref. [21] for $d+(t\mu)$. While there are some small disagreements, the overall comparison is quite good. The $L=1$ partial wave cross section for $d+(d\mu)$ elastic scattering from threshold to 10 eV is shown in Fig. 8 and the corresponding cross section for $d+(t\mu)$ from 0 to 100 eV is shown in Fig. 9. Gross qualitative differences exist between the Born-Oppenheimer results and the precise three-body calculations. Clearly the missing Born-Oppenheimer (1,1) bound state in $d-d-\mu$ has appeared as a scattering resonance at about 2–3 eV (5 eV above its true position) with a width that is comparable. For the $d+(t\mu)$ scattering the opposite effect is visible. The precise calculations give a much larger $L=1$ cross section than does the Born-Oppenheimer approximation. This can be traced to the fact that the (1,1) bound state actually appears just below threshold ($E=-0.66$ eV), while it is at -7.8 eV in the Born-Oppenheimer approximation.

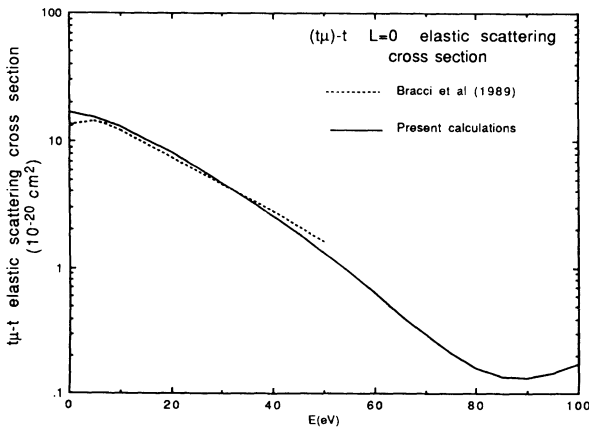


FIG. 7. Comparison of spin-averaged $L=0$ elastic scattering cross section for $t+(t\mu)$ in the Born-Oppenheimer approximation with accurate three-body results. Solid curve, present calculations; dotted curve, Ref. [20].

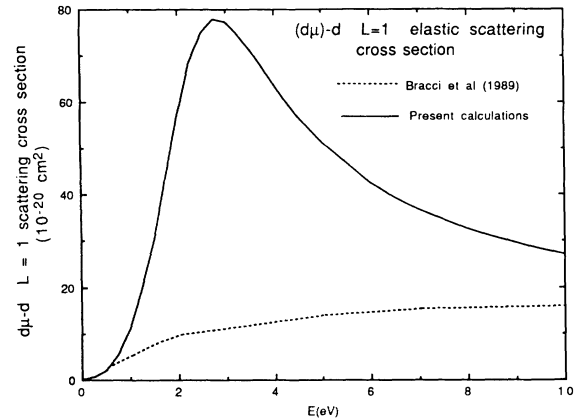


FIG. 8. Comparison of spin-averaged $L=1$ elastic-scattering cross section for $d+(d\mu)$ in the Born-Oppenheimer approximation with accurate three-body results. Solid curve, present calculations; dotted curve, Ref. [20]. The weakly bound (1,1) state at -1.975 eV, absent in the Born-Oppenheimer approximation, manifests itself instead as a resonance a few eV above threshold.

IV. ANALYTICITY OF PARTIAL-WAVE AMPLITUDES AND $k^{2L+1}\cot\delta$ EXPANSION

It is well known [27] that partial-wave scattering amplitudes in potential scattering have certain analytic properties in the complex k and E planes: bound-state poles on the positive imaginary axis in the k plane, possible conjugate poles in the lower half k plane (with the same imaginary part, but opposite real parts), leading to bound-state poles on the negative real energy axis on the first Riemann sheet and resonance poles reached through the positive energy cut, on the second sheet. For multichannel scattering, the sheet structure is more complicated, but the general behavior is the same.

Unitarity implies that $F_L = k^{2L+1}\cot\delta_L$ is a real mero-

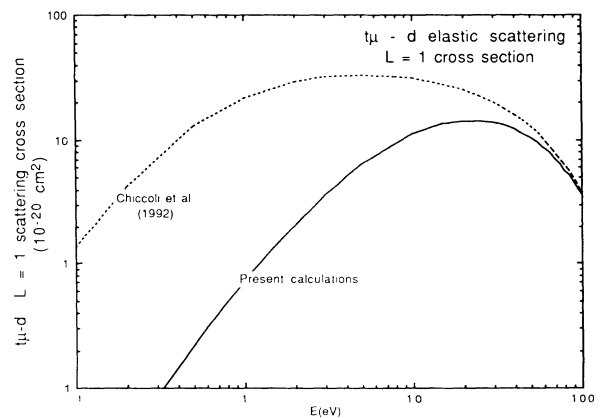


FIG. 9. Comparison of spin-averaged $L=1$ elastic-scattering cross section for $d+(t\mu)$ in the Born-Oppenheimer approximation with accurate three-body results. Solid curve, present calculations; dotted curve, Ref. [21]. The weakly bound (1,1) state at -0.66 eV is close enough to threshold to enhance the accurate p -wave scattering. In the Born-Oppenheimer calculations the bound state is at -7.82 eV, further away.

morphic function of E or of k^2 . Poles of the scattering amplitude in the k -plane are defined by $\cot\delta=i$, or $F_L(k^2)=ik^{2L+1}$. With the definition $k=iz$, the relation reads $F_L(-z^2)=(-1)^{L+1}z^{2L+1}$, an equation with real coefficients if F_L is represented by a finite polynomial in k^2 . Then most of the stated analytic properties can be seen to follow directly from the properties of the roots of a polynomial with real coefficients.

To illustrate the use of the analyticity of $k^{2L+1}\cot\delta$ to determine pole parameters, we take the Born-Oppenheimer numerical results for the gerade phase shift for the $L=1$ d -($d\mu$) partial wave and make a polynomial fit in k^2 to $F_L(k^2)$. Figure 10 shows the behavior of $k^3\cot\delta$ as a function of k^2 . The range corresponds to 0–10 eV, as in Fig. 8. The vanishing at $E=4.3$ eV shows where the real phase shift goes through 90° , but for a broad resonance the pole may be some distance away. On the 0–10 eV energy range, elementary polynomial fits to $F_1(k^2)$ with power series in k^2 up to $(k^2)^N$ for $N=2$ and 3 were generated with CricketGraph software. A complex Newton's method found the roots in the k plane. The results for $N=3$ are displayed in Fig. 11. Note the pair of complex poles near the real axis. The right-hand one is the resonance near the real E axis on the second sheet. It has parameters $E_{\text{res}}=1.98$ eV, $\Gamma=-2\text{Im}E=2.82$ eV. For $N=2$, not shown, there are four poles: the two conjugate poles at almost exactly the same positions as for $N=3$, and two on the positive imaginary axis just as for $N=3$, although not quite in the same positions. The latter two, apparently bound states, are actually spurious, resulting from the approximation of $k^3\cot\delta$ by a polynomial on a finite interval. Any pole located a distance from the origin comparable to or larger than the range over which $k^{2L+1}\cot\delta$ is approximated (in this case, out to $|k|=0.18$) should be viewed with suspicion. The closest “bound-state” pole is at $k=i0.19$. Similarly, for $N=3$, the additional pair of conjugate poles in the lower half of the k plane are extremely remote, far outside the range of plausibility. The lesson here is that higher-order polynomial fits are only

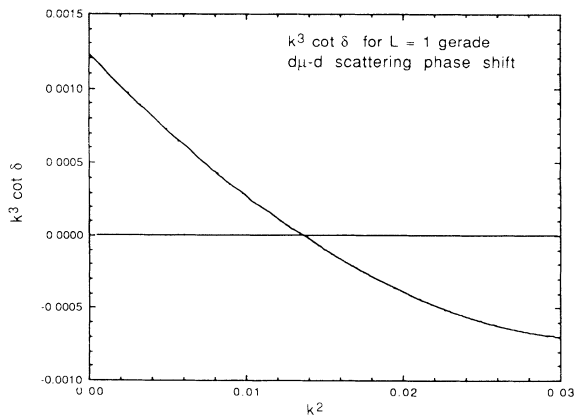


FIG. 10. $k^3\cot\delta$ for the $d+(d\mu)$, $L=1$ gerade scattering phase shift as a function of k^2 corresponding to energies from 0 to 10 eV. The phase shift goes through $\pi/2$ at 4.3 eV. See text for discussion.

useful to confirm the stability of the “nearby” pole or poles found with the polynomial of least reasonable degree. The higher the degree, the more the number of spurious poles.

A test of the location of a true bound state through use of scattering information is afforded by the amplitude tabulations in Ref. [21]. Table 11 there gives values of t_{11} for the $L=1$ partial wave in d -($t\mu$) scattering. This amplitude can be identified with $\tan\delta_{g0}$, even though, according to Eq. (3), there is a (small repulsive) contribution from the ungerade potential. In a search for a bound state in the attractive gerade potential, the admixture is irrelevant. An $N=3$ polynomial fit to k^3/t_{11} from 0 to 35 eV [below the $t+(d\mu)$ threshold at 42.8 eV] results in two poles close to the origin, one at $E=-0.624$ eV on the first Riemann sheet and one at $E=-0.423$ eV on the second sheet. Four other poles are near the edge or beyond the region of the approximation to $k^3\cot\delta$ and

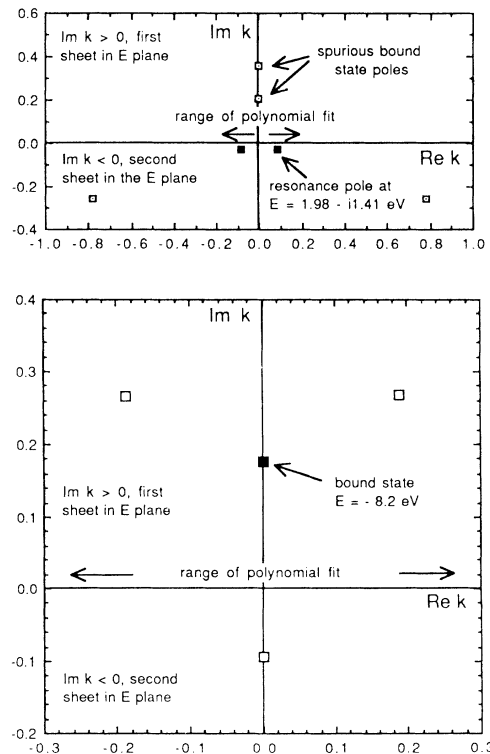


FIG. 11. (Top) Poles of the $L=1d+(d\mu)$ elastic-scattering amplitude in the complex k plane, based on a polynomial fit of degree 3 in k^2 to the numerical data represented in Fig. 10. The range of k values involved in the fit is indicated by the arrows. Physically significant are the two poles near the origin, corresponding to a resonance on the second Riemann sheet at $(\text{Re},E,\text{Im}E)=(1.98,-1.41)$ eV and its partner. The other poles, at the edge of or beyond the “circle of confidence” defined by the range of the fit, are spurious artifacts of the polynomial representation. (Bottom) Corresponding poles for the $L=1$ $d+(t\mu)$ scattering amplitude in the Born-Oppenheimer approximation (Fig. 9), from a quadratic polynomial fit in k^2 to $k^3\cot\delta$ from 0 to 20 eV. The bound state pole is inferred from the scattering amplitude to be at -8.2 eV, close to the actual computed value of -7.82 eV.

are judged spurious. The bound state at -0.660 eV shows up clearly in the scattering amplitude. Another fit, this time with $N=2$ and only from 0 to 2 eV, yields virtually the same two poles near the origin (-0.675 and -0.433 eV) and two very remote.

The corresponding comparison for the Born-Oppenheimer approximation is shown in the bottom part of Fig. 11, where the poles of the $L=1$ scattering amplitude for the $d+(t\mu)$ gerade potential are shown, based on an $N=2$ polynomial fit to $k^3 \cot \delta$ on the energy range 0–20 eV. The bound state pole is at $E=-8.2$ eV, compared with $E=-7.82$ eV by direct computation (in the Born-Oppenheimer approximation). There are also a “virtual state” at $E=-2.3$ eV and two spurious poles.

V. THE $L=3$ RESONANCE AND THE SEARCH FOR $L=0$ RESONANCE AT 54 eV

Higher partial waves are important in the process of establishing the trustworthiness of the Born-Oppenheimer approximation as a description of the physics involved and the expected magnitudes of parameters (such as resonant widths). Of particular interest is the $L=3$ partial wave in $d-(t\mu)$ scattering. The calculations of Ref. [21] (Table 26 and Fig. 26) show a narrow resonance at 22 eV. Inspection of the $d-t-\mu$ effective radial potential-energy curves shown in Fig. 12 for the gerade ground state show the reason. The $L=3$ potential is deep enough to yield a quasibound state, yet has enough of a shoulder partially to “trap” the nuclear motion and give a narrow width. The $L=2$ potential is deep enough to have a true bound state, with insufficient shoulder to make a scattering resonance. The $L=4$ potential is too shallow to give resonant behavior.

A calculation of the $d-(t\mu)$ $L=3$ effective scattering cross section by the gerade potential is compared with the accurate calculations of Ref. [21] in Fig. 13. In our approximation of mass degeneracy in computing the phase shifts and cross sections, with the neglect of a small

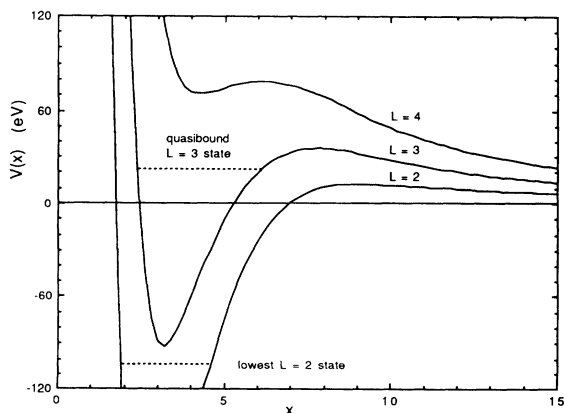


FIG. 12. Effective $n=1$ potential-energy curves of radial motion for the $d-t-\mu$ system for $L=2, 3$, and 4. The energies are in eV and the radius in units of a_μ . The $L=3$ potential is sufficiently attractive at intermediate distances to support one “bound” state and sufficiently repulsive at larger distances to give it a relatively narrow width.

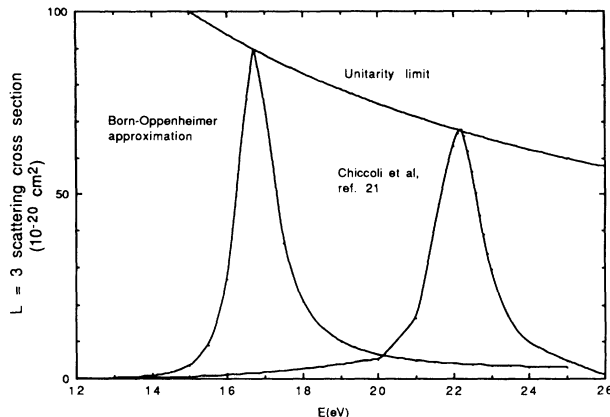


FIG. 13. The $L=3$ elastic-scattering cross section for energies between 12 and 26 eV, showing the resonance at 22.2 eV with a width of 1.4 eV bound in the calculations of Ref. [21] along with the resonance in the Born-Oppenheimer approximation at 16.7 eV with a width of 1.2 eV.

contribution from the negative shift in the ungerade scattering amplitude, the cross section according to Eq. (3) would be $\frac{1}{4}$ of what is shown in Fig. 13. We plot the full gerade cross section for clearer comparison with the accurate results, which describe the purely elastic scattering in the channel $d+(t\mu) \rightarrow d+(t\mu)$, the channel $t+(d\mu) \rightarrow t+(d\mu)$ being closed at these energies. The Born-Oppenheimer approximation gives the location of the resonance at $E_0=16.7$ eV, with a width of $\Gamma=1.2$ eV, while the accurate values are $E_0=22.18$ eV and $\Gamma=1.39$ eV. The discrepancy of 5.5 eV in position is typical; the slightly smaller width is a reflection of the lower resonant energy and the consequent thicker potential barrier.

Two remarks are warranted: Display of the wave functions of the scattering process at different energies across the resonance provides vivid reality to the idea of a quasistationary state. The peak probability density inside the potential well relative to the asymptotic density nicely follows a Breit-Wigner resonant shape. Figure 14 shows the squares of the radial wave functions at two energies, on resonance ($E=16.75$ eV) and off ($E=15$ eV), normalized to the same magnitude at large distances. The second remark is that application of semiclassical WKB techniques can give qualitatively correct values for the resonant energy and width. Use of the quantization condition

$$(n - \frac{1}{2})\pi = \int_a^b k(x) dx, \quad (7)$$

where $n=1, 2, 3, \dots$, a and b are the classical turning points, and $k(x)$ is the radial wave number $k^2(x) = (2M/\mu)[E - V_{\text{eff}}(x)]$ gives an energy of 22.9 eV for the lowest state in the $L=3$ gerade potential. The width can be estimated as follows. The classical period of radial oscillation is given by twice the integral of $1/v(x)$ between a and b . In muonic hartree units, we have

$$\frac{\tau}{\tau_0} = \left[\frac{2M}{\mu} \right]^{1/2} \int_a^b \frac{dx}{\sqrt{E - V_{\text{eff}}(x)}}, \quad (8)$$

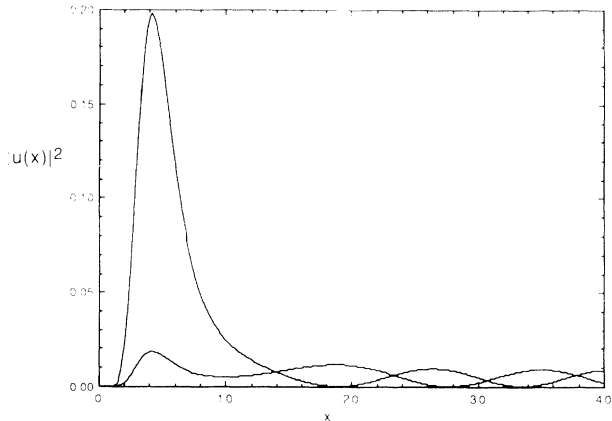


FIG. 14. Squares of two $L=3$ radial scattering wave functions $[|u(x)|^2=4\pi r^2|\psi(r)|^2]$, normalized at large distances to the same average value. The upper curve is at resonance, $E=16.7$ eV; the lower curve is for $E=15$ eV. The quasistationary nature of the resonant state is clearly demonstrated.

where $\tau_0 = \hbar a_\mu / e^2$. The inverse of the classical period is an estimate of the rate of attempts by the reduced particle to escape through the barrier. Multiplication by a Gamow penetration factor $\exp[-2 \int \kappa(x) dx]$ for the barrier gives an estimate of the width. The classical oscillation frequency corresponds to a width of 10 eV; the barrier penetration factor is 0.368 at 22.9 eV; the width is thus $\Gamma_{\text{WKB}} \approx 3.7$ eV. Because the barrier is relatively “thin,” the simple-minded Gamow factor is not expected to give more than qualitative results. In the event, it is in error by a factor of 3.

We now turn to the search within the Born-Oppenheimer approximation for poles in the $L=0$, $d+(t\mu)$ scattering amplitude for the gerade ground-state potential, in particular, for the reported pole at $E=(54.35-i0.37)$ eV. The phase shifts were calculated

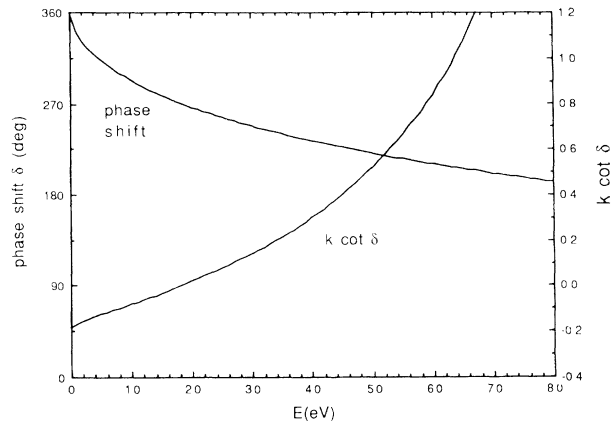


FIG. 15. The phase shift in degrees (left-hand scale) and $k \cot \delta$ (right-hand scale) for the scattering in the $L=0$ gerade potential of the $d+(t\mu)$ system as functions of energy from 0 to 80 eV. See text for discussion.

from 0 to 100 eV in 1.0-eV steps. The phase shift in degrees and $ka_\mu \cot(\delta)$ are shown as functions of energy in Fig. 15. The phase shift falls monotonically from 2π at zero energy (reflecting the two $L=0$ bound states) through $3\pi/2$ at $E \approx 18$ eV and on towards π at roughly 96 eV. A narrow resonance would cause the phase shift to increase abruptly by nearly 180° across the resonant energy before declining again at higher energies. There is no sign of any such structure that would indicate the presence of a resonant state anywhere on the interval. A finer-grained search was made between 40 and 60 eV with no change in conclusion. Despite the absence of any hint in the behavior of the phase shift of a narrow state, one can apply the approach of Sec. IV and search for poles in the complex k or E plane. An $N=5$ polynomial fit to $k \cot \delta$ on the integral $(0, 75)$ eV yields ten complex poles on the two Riemann sheets:

$$(\text{Re}E, \text{Im}E) = \left\{ \begin{array}{l} (-0.64, \pm 9.1); (23.3, \pm 26.3); (67.0, \pm 31.3) \text{ (first sheet)} \\ (-3.4, \pm 28.2); (64.2, \pm 42.4) \text{ (second sheet)} \end{array} \right\}.$$

None of these poles has a width $\Gamma (=2 \text{Im}E)$ less than 18 eV. Furthermore, all but the first pair on the second sheet are suspect. Poles on the first sheet represent bound states and should not occur in pairs; the second pair on the second sheet is near the limit of the range of fitting of $k \cot \delta$. Since the phase shift passes through π at 96 eV, giving a pole in $k \cot \delta$, this singularity was fitted numerically and the difference with $k \cot \delta$ was approximated by a $N=5$ polynomial in k^2 on the range up to 85 eV. The scattering amplitude now yielded 12 poles:

$$(\text{Re}E, \text{Im}E) = \left\{ \begin{array}{l} (-2.4, \pm 12.3); (24.7, \pm 36.4); (84.9, \pm 43.7); (139.1, \pm 4.5) \text{ (first sheet)} \\ (-10.9, \pm 44.2); (90.6, \pm 60.2) \text{ (second sheet)} \end{array} \right\}.$$

Apart from the additional pair on the first sheet (far outside the plausible region), the five pairs can be seen to correspond to the earlier fit without the singularity in $k \cot \delta$.

Having failed to find the reported narrow resonances (also not seen in the scattering calculations of Ref. [21], incidentally, nor in the calculations of Ref. [28]), we address the plausibility of such a narrow state in the s wave

or p wave at such an energy. We saw in Sec. III that the energy of the $d-d-\mu(1,1)$ state is slightly positive in the Born-Oppenheimer approximation, rather than slightly negative. The shift is about 4 eV, putting it as an $L=1$ resonance at $(\text{Re}E, \text{Im}E) = (2.0, -1.4)$ eV. The width is $\Gamma = 2.8$ eV. If such a state were at 50 eV instead of 2 eV, it would have a width so large as to make the idea of a resonance inapplicable. The $L=1$ centrifugal barrier is

just not large enough to keep the width small as the energy increases. Similarly, the $L=3$ resonance of Ref. [21] and found in our calculations has a smaller width ($\Gamma \approx 1.4$ eV) at 22 eV because of the higher centrifugal barrier, but would have considerably larger width if its energy were at even 40 eV (see Fig. 12). The reported states in $L=0$ and 1 at $E \approx 54$ eV have widths of 0.74 and 2.04 eV. Since there is no centrifugal barrier in $L=0$ and only a very weak one in $L=1$, widths of the order of 1 eV are counterintuitive.

The accurate three-body wave functions can be written as expansions in Born-Oppenheimer eigenstates of the molecular potential energies of the different electronic orbitals. The presence in our approximation of only the one wave function, corresponding to the $1s \sigma_g$ muonic configuration, is what has led to the statement that narrow continuum states can only appear in the complete three-body calculations. Already in the Introduction we had pointed out that the one-muon-two-nuclei molecule is too simple a system to give rise to Feshbach resonances [14,15]. In the language of linear combinations of Born-Oppenheimer states, the nonzero muon mass and the different masses for nonidentical nuclei mix the gerade and ungerade states for the lowest electronic orbital as well as mixing in other excited orbitals. The latter lie roughly 2 keV above the lowest potential-energy curves and presumably do not enter decisively. It is difficult to see how an admixture of the repulsive $2p \sigma_u$ state and small amounts of energetically distant states could produce a narrow continuum resonance that the authors describe as a member of the sequence of vibrationally excited $L=0$ states [9].

Another related point is the existence of the $t+(d\mu)$ threshold at 48 eV. The claimed narrow resonances are 6 eV above this threshold. While it is known that the separation of degenerate thresholds by symmetry breaking can cause complicated motions of resonances [29,30], it does not appear likely that a remote pole would migrate to a position only 1 eV from the real axis because of a threshold 6 eV away. Even if, for some reason, it was appropriate to think of the kinematics of decay for these resonances in terms of the energy above the $t+(d\mu)$ threshold, the absence of a centrifugal barrier makes 6 eV quite high enough to cause an s -wave width much larger than 6 eV: witness the $d-d L=1$ resonance at 2 eV with a width of 2.8 eV.

VI. $n=2$ RESONANCES

A large number of continuum resonances in the $d-t-\mu$ system associated with the $d+[t\mu(2s)]$ threshold, roughly 2110 eV above the lowest threshold, have been reported and their properties examined [10–13,16]. As pointed out by Shimamura [16], the Born-Oppenheimer approximation is an excellent approximation for these states. The lowest-lying $n=2$ potential energy at intermediate distances is the $3d \sigma_g$ curve shown in Fig. 1. The potential minimum is at larger r than for $n=1$ and is much shallower. There is an attractive tail on all the $n=2$ gerade potentials from the first-order “Stark effect,” $\Delta V = -3/x^2$. Simple WKB arguments show that

in such circumstances there is an infinite number of bound states for small L values, with binding energies going as $|E_\nu| \approx C \exp(-\beta\nu)$, where ν is the vibrational quantum number and $\beta = 2\pi(\mu/6M)^{1/2}$. Atomic screening will cut off the x^{-2} potential, of course, and limit the sequence of bound states. For the $d-t-\mu$ system, $\nu_{\max} \lesssim 9$.

The results of our Born-Oppenheimer calculations are compared to the more elaborate calculations in the tables below. There is an issue of the crossing of potential-energy curves of the same symmetry. As can be seen in Fig. 1, for $x < 4$ the $2s \sigma_g$ curve lies below the $3d \sigma_g$. In the complete adiabatic limit, the motion is “classical” and follows the lowest potential-energy path. Nonadiabatic behavior tends to cause the system to go rapidly past the crossover point without changing from one curve to the other. For the states discussed here, the differences in energies are less than 1 eV when the potential is changed from being $3d \sigma_g$ at all distances to following the $2s \sigma_g$ curve for $x < 4$ because the classical turning points are always outside $x=4$. With appreciable departure from adiabatic behavior there will, of course, be significant mixing of different muonic orbital Born-Oppenheimer states. Whether such admixtures can plausibly produce some of the properties claimed for these states is discussed below.

In Table I we compare the Born-Oppenheimer energies for the $L=0$ and 1 bound states, i.e., states lying below the $d+t\mu(2s)$ threshold, with the calculations of Refs. [10–13]. Differences of the order of 10–15 eV are apparent, while there is general agreement (to 0.7 eV or less) among the accurate calculations [31]. The differences in energy between state of $L=1$ and 0 for the same radial quantum number are reasonably well given by the Born-Oppenheimer approximation, as might be expected, since the mean value of r^{-2} is dominated by the classically allowed region where the mean square wave function is not far from the Born-Oppenheimer form.

Of considerably more interest are the comparisons of Table II. The first point to be made is that the more elaborate three-body calculations and the Born-Oppenheimer approximation yield closely similar results for properties of the wave function in the classically allowed region [32]. The second and third columns of Table II show the comparison between the mean nuclear separations for the first four $L=0$ states. The squares of Born-Oppenheimer and pseudo-wave-functions agree well in the classically allowed region [33]. The average value of the Born-Oppenheimer wave function in that region (column 4 of Table II) can therefore be taken as the approximate average of the three-body pseudo-wave-function as well. Columns 5 and 6 demonstrate a characteristic of the Born-Oppenheimer approximation. Because of the penetration to the origin through a very thick Coulomb barrier, the square of the wave function at the origin is exponentially small—by factors of 10^{12} , typically—compared to the average $\langle |\psi(x)|^2 \rangle$ in the classically allowed region. In contrast, the results of Refs. [12] and [13] in columns 7 and 8 for the nuclear densities at zero internuclear separation, while differing among themselves, are huge by comparison. Comparison of column 7 with column 4 shows that the Coulomb

TABLE I. Comparison of energies of $n=2$ d - t - μ continuum resonances for $L=0$ and 1 with numerical three-body calculations. Energies are in eV, relative to the d -($t\mu$, $n=2$) energy. BO denotes Born-Oppenheimer.

L, v	E_{BO}	Ref. [10]	Ref. [11]	Ref. [12]	Ref. [13]	$E(1, v) - E(0, v)$ (BO)	$E(1, v) - E(0, v)$ (Ref. [10])
0,0	-234.5	-217.892	-217.870	-217.892	-217.889		
1,0	-228.4	-212.547	-212.511			6.1	5.345
0,1	-151.5	-139.724	-139.502	-139.731	-139.705		
1,1	-146.5	-135.375	-135.146			5.0	4.349
0,2	-86.4	-79.095	-79.385	-79.118	-78.937		
1,2	-82.5	-75.675	-74.940			3.9	3.421
0,3	-41.6	-36.567		-36.610			
1,3	-38.9	-34.233	-33.395			2.7	2.334

repulsion causes only a factor of 40 reduction in probability for the (0,0) state, a factor of 4 for the (0,1) state, and a factor of 3 for (0,2) state. The larger value of the probability at the origin than the value in the classically allowed region for the (0,3) state seems especially suspect. The corresponding factors for the first three states from Ref. [13] are 2000, 100, and 20.

The drastically different behaviors of our wave functions and the pseudo-wave-functions in the classically forbidden interior region demands discussion. Examination of Fig. 1 shows that, in the framework of the Born-Oppenheimer approximation, the Coulomb barrier extends from the origin out to $x \approx 7$ for the $n=2$ states and only out to $x \approx 1.7$ for $n=1$. For the $n=1$ ground state, the ratio $|\psi(0)|^2$ to $\langle |\psi(x)|^2 \rangle$ is roughly $\frac{1}{3600}$ and is not different by a factor of 2 between the Born-Oppenheimer and accurate three-body calculations. The tiny results of Table II for $|\psi(0)|^2$, while perfectly understandable within the Born-Oppenheimer approximation, are surely underestimates. There are many muonic orbital configurations besides the $3d \sigma_g$ (not shown in Fig. 1) that may contribute to the wave functions. Nevertheless, the results of Refs. [12] and [13] seem extreme in the other direction. The pseudo-wave-function for the $n=2$ (0,0) state, while agreeing with the Born-Oppenheimer wave function in the classically allowed region, departs markedly for $x < 4$, exhibiting rapid oscillations (an interior ‘‘classically allowed’’ region) that indicate a large positive local kinetic energy of nuclear motion [33]. At $x \approx 2.0-2.5$, the local wavelength implies an average

kinetic energy of about 0.23 muonic hartree units and at $x \approx 0.5-1.2$, roughly 0.42 muonic hartree units. Such large positive local kinetic energies at $x < 3$ implies great departure of the three-body wave function from the dominant Born-Oppenheimer component that governs the behavior at larger radii. Inspection of Fig. 1 indicates that at these close distances the $n=2$ (0,0) three-body wave function would necessarily have a major, even dominant, admixture of the $n=1$ ground state. This inference is consistent with Table III of Ref. [13]. A decomposition of the three-body wave function at zero internuclear separation into heliumlike atomic states shows 42% probability each for the atomic $1s$ and $2s$ states, with 5.5% probability for $3s$ and smaller percentages for higher states (the whole helium-like continuum contributes 8.8%). The appreciable amount of $2s$ is understandable from Fig. 1; the $2s \sigma_g$ potential energy lies lower than the $3d \sigma_g$ curve for $x < 4$, as mentioned in the second paragraph of this section. An equal amount of the $1s$ configuration seems somewhat surprising. It is believed not to be an artifact of the variational trial wave functions [33].

VII. SUMMARY AND CONCLUDING REMARKS

The Born-Oppenheimer approximation provides, in my view, a useful exploratory tool for muonic molecular-ion dynamics. As Figs. 2–7 show, it provides a semiquantitative description of both bound states and low-energy s -wave scattering. It fails, of course, to give the finer details, such as the slightly bound (1,1) states in the d - d - μ

TABLE II. Comparison of present results for the mean separation of the nuclei $\langle x \rangle$ and $|\psi(0)|^2$ with the equivalent results of Refs. [12] and [13]. The mean nuclear separation is in units of a_μ . The column $\langle |\psi(x)|^2 \rangle$ contains the average value of the square of the Born-Oppenheimer wave function of nuclear motion between the classical turning points in units of 10^{26} cm^{-3} . The density of nuclei at zero internuclear separation is in the same units. The two columns of $|\psi(0)|^2$ correspond to the use of (i) the $3d \sigma_g$ potential for all x and (ii) the use of the $3d \sigma_g$ potential for $x > 4.05$, but the softer $2s \sigma_g$ potential inside $x = 4.05$. The final columns give the corresponding density $\rho_N(0)$ from the three-body calculations of Refs. [12] and [13], as deduced from the stated values of the fusion rate.

L, v	$\langle x \rangle$ (BO)	$\langle x \rangle$ (Ref. [12])	$\langle \psi(x) ^2 \rangle$	$ \psi_1(0) ^2$	$ \psi_2(0) ^2$	$\rho_N(0)$ (Ref. [12])	$\rho_N(0)$ (Ref. [13])
0,0	9.8	9.83	103	1.5×10^{-12}	2.6×10^{-11}	2.4	0.054
0,1	11.7	11.87	41.1	7.1×10^{-12}	1.4×10^{-10}	10.8	0.407
0,2	14.3	14.85	20.2	1.6×10^{-11}	3.1×10^{-10}	6.0	0.922
0,3	18.4	20.92	9.22	2.1×10^{-11}	4.3×10^{-10}	135.0	

and d - t - μ systems. The failure to describe accurately these states near threshold reflects itself in a disagreement with the accurate three-body calculations for low-energy p -wave scattering (Figs. 8 and 9). Even there, an $L=1$ resonance at 2 eV above threshold for d - d - μ can be viewed as semiquantitative agreement with the accurate bound state at -1.975 eV. The width of 2 or 3 eV for that p -wave state and the width of 1.4 eV for the $L=3$ resonance at 22 eV above threshold (found 5 eV away in the Born-Oppenheimer approximation) set the scale for expected widths of resonances as functions of energy and centrifugal barrier. Examination of the d - t - μ gerade s -wave phase shift itself and a search for poles of the S matrix through the $k \cot \delta$ expansion give no indication of a narrow resonance near 50–60 eV above threshold [8,9], or indeed any resonance at all.

The family of d - t - μ continuum resonances 1.9 keV above threshold are known [16] to be “ordinary” molecular states based on the $3d \sigma_g$ electronic potential-energy curve (see Fig. 1). To the extent that the $n=2$ t - μ atom can be viewed as a stable species, these states are true bound states, lying below the d - t - μ ($n=2$) threshold. The Born-Oppenheimer approximation provides a semiquantitative description of the energy levels and wave functions. Tables I and II summarize the results. Comparison of our calculations with those of Refs. [12] and [13] shows rough agreement for properties that depend upon the integrated wave function or the wave function in the classically allowed region. Understandable disagreement occurs for quantities such as $\rho_N(0)$, where the mixing of different electronic configurations is presumably important. Nevertheless, even the smaller values of $\rho_N(0)$ reported in Ref. [13] seem excessively large, making the fusion rates and widths quoted there somewhat suspect.

Assuming the properties of the $n=2$ continuum resonances are known, one can ask whether they enter importantly in the cycle of muonic catalysis. The $n=2$ t - μ atomic states are certainly formed in the process of cascade to the ground state by collisions and radiative transitions. For liquid densities, estimates [34,35] are that roughly 15% of the atoms arrive at the $2s$ state. The Day-Snow-Sucher effect [36] in the collisions will cause Stark mixing of the $t\mu(2s)$ state with the $t\mu(2p)$ state. For kinetic energies larger than the fine structure (0.2–0.3 eV), the $2s \rightarrow 2p$ mixing rate is of the order of 10^{13} s^{-1} at liquid-hydrogen density [35]; at thermal energies the rate (for radiative collisional deexcitation) drops to of the order of $2 \times 10^{10} \text{ s}^{-1}$ [37]. The rate for the radiative $2p \rightarrow 1s$ transition is $1.3 \times 10^{11} \text{ s}^{-1}$. *A priori*, the fusion rates of Ref. [13], (10^{11} – $2 \times 10^{12} \text{ s}^{-1}$) would imply that some fusion via these states might occur, *provided* the molecules could be formed. The terminology “continuum resonances” is misleading in this regard. As we have said, these $n=2$ molecular states are *bound* states as far as the d - t - μ ($n=2$) channel is concerned. They are not resonances in that channel. The rates of molecular formation may be enhanced somewhat by their large sizes, but the formation will not be by the Vesman mechanism but by Auger emission with Q values of up to 217 eV. The molecular formation cross sections will be very small. Only for the states with vibrational excitation

$7 \leq v \leq v_{\max} = 9$ (binding energies less than 4 eV) is there any remote chance of an appreciable cross section of molecule formation by the Vesman mechanism. These states are so large in size [38] that their undisturbed existence inside electronic molecules is in doubt. In any event, currently there is no information on the fusion or other rates for such highly excited and diffuse states.

ACKNOWLEDGMENTS

I thank J. S. Cohen, M. Leon, L. I., Ponomarev, and K. Szalewicz for helpful discussions and comments on a draft, and P. Froelich for his generous interactions by electronic mail and by FAX on the subject of the $n=2$ resonances. This work was supported by the Director, Office of Energy Research, Office of High Energy and Nuclear Physics, Division of High Energy Physics of the U.S. Department of Energy under Contract No. DE-AC03-76SF00098.

APPENDIX: ANALYTIC APPROXIMATIONS TO THE “ELECTRONIC” ENERGIES

The following table gives the polynomial (or other) interpolation and extrapolation formulas fitted to the numerical results of Bates, Ledsham, and Stewart [22] for the electronic energies of the hydrogen molecular ion in the Born-Oppenheimer approximation. The energies are labeled with the same convention as used by Bates, Ledsham, and Stewart, but the energies are in atomic units rather than rydbergs. The zero of energy is taken in each case to be that of a neutral hydrogen atom and a $Z=1$ nucleus at infinite separation, i.e., $E_\mu(x) = E_e(x) - E_e(\infty)$. For the $n=1$ group of molecular states, the atom is in its $1s$ state when at large separations; for the $n=2$ group (continuum resonances), the atom is in the $n=2$ atomic state. Asymptotically, the electronic energies are fitted to a form that gives rise to the quadratic ($n=1$ group) or linear ($n=2$ group) Stark potentials when added to the Coulomb repulsion between the nuclei. For the $n=1$ group, the potential goes as $V(x) \rightarrow -9/4x^4$, while the $N=2$ potential goes as $V(x) \rightarrow -3/x^2$.

For the range of x spanned by the tables of Bates, Ledsham, and Stewart ($0 \rightarrow 9$ or 10), the electronic energies are fitted over portions of the range by inverse polynomials. The segmentations are arbitrary; they were chosen by trial and error in an effort to obtain a reasonable representation with polynomials of modest degree. Beyond the range of the numerical tables of Bates, Ledsham, and Stewart, an arbitrary form is used to bridge from the tables at their largest x to the known Stark effect form at very large x . Where possible these forms are chosen to agree closely with the exact computations of Madsen and Peek [23] on the range $10 < x < 50$.

$$n = 1$$

$1s \sigma_g$ state

The “electronic” energy is written as $E_\mu(x) = -1.5/P(x)$, with $P(x) = a_0 + a_1x + a_2x^2 + a_3x^3 + a_4x^4$.

Coefficient	$0 < x < 2.5$	$2.5 < x < 9$
a_0	1.0	1.928 3
a_1	0.227 28	-0.414 15
a_2	0.494 89	0.427 27
a_3	-0.170 35	-0.035 998
a_4	0.026 669	0.001 033 8

For $x > 9$, the function $P(x)$ is

$$P(x) = 1.5x^4 \left[x^3 + 2.25 - \frac{175.8165}{x^2} + \frac{53\,205.69}{x^4} \right]^{-1}.$$

Comparison of the fit for the $1s \sigma_g$ state (without the Coulomb repulsion) with the Born-Oppenheimer energies in Table II of Struensee, Cohen, and Park [24] ($x = 0.1-25$) shows agreement to a few parts in 10^3 for $0.3 < x < 2.0$ and considerably better for $2 < x < 25$. Such accuracy is adequate for our purposes.

$3p \sigma_u$ state (called by others the $1 \sigma_u$ or the $2p \sigma_u$ state)

The “electronic” energy is written as $E_\mu(x) = -x^2/Q(x)$, with $Q(x) = b_0 + b_1x + b_2x^2 + b_3x^3$.

Coefficient	$0 < x < 3$	$3 < x < 9$
b_0	15.602	-1.7798
b_1	-3.1534	12.687
b_2	2.3474	-2.4176
b_3	0.64674	1.1188

For $x > 9$, the function $Q(x)$ is

$$Q(x) = \frac{4x^6}{4x^3 + 9 \left[1 - \left(\frac{10.3625}{x} \right)^6 \right]}.$$

$n = 2$

Here we only tabulate fits for the even states (which give attractive potentials for nuclear motion). There are two, the $3d \sigma_g$, which lies lowest at large x , and the $2s \sigma_g$, which lies below the $3d \sigma_g$ state for $x < 4.05$.

$3d \sigma_g$ state (called by others the $3 \sigma_g$ state)

The potential energy is needed at quite large distances, especially for the higher vibrational states. The following segments give an adequate representation for $0 < x < 50$.

(a) For $0 < x \leq 5$ the “electronic” energy is written $E_\mu(x) = -7/[72P(x)]$, where

$$P(x) = 1.0006 - 1.7378(-2)x + 8.2391(-3)x^2 - 2.7605(-2)x^3 + 7.1911(-3)x^4 - 5.2048(-4)x^5.$$

(b) For $5 < x \leq 14$, $E_\mu(x) = -[3/x^2 + p(x)]$, where

$$p(x) = -1.2718 + 0.619\,14x - 0.108\,21x^2 + 9.4249(-3)x^3 - 4.1341(-4)x^4 + 7.2909(-6)x^5.$$

(c) For $14 < x \leq 25$, $E_\mu(x) = -[3/x^2 + 1/x + q(x)]$, where

$$q(x) = -3.2718(-2) + 1.6359(-2)x - 1.5763(-3)x^2 + 5.7049(-5)x^3 - 7.1917(-7)x^4.$$

(d) For $x > 25$, $E_\mu(x) = -[3/x^2 + 1/x + 1/r(x)]$, where $r(x) = -6.3035x^2 + 0.33842x^3 - 1.8752(-3)x^4$.

$2s \sigma_g$ state

We only give the fit for $x < 4.05$, where the “electronic” energy is lower than that of the $3d \sigma_g$ state. The form for $E_\mu(x)$ is the same as for the $3d \sigma_g$ state, but for $x < 4.05$ the function $P(x)$ is $P(x) = \frac{7}{27}p(x)$ where $p(x) = 0.989\,91 + 0.1977x + 0.089\,179x^2 - 0.023\,633x^3 + 0.002\,332\,567x^4$.

- [1] L. I. Ponomarev, *Contemp. Phys.* **31**, 219 (1990).
- [2] J. D. Jackson, *Phys. Rev.* **106**, 330 (1957).
- [3] S. E. Haywood, H. J. Monkhorst, and K. Szalewicz, *Phys. Rev. A* **37**, 3393 (1988).
- [4] M. Struensee and J. S. Cohen, *Phys. Rev. A* **38**, 44 (1988).
- [5] C. D. Stodden, H. J. Monkhorst, K. Szalewicz, and T. G. Winter, *Phys. Rev. A* **41**, 1281 (1990).
- [6] S. A. Alexander and H. J. Monkhorst, *Phys. Rev. A* **38**, 26 (1988).
- [7] I. V. Puzynin and S. I. Vinitsky, *Muon Catalyzed Fusion* **2**, 207 (1988).
- [8] P. Froelich and K. Szalewicz, *Phys. Lett. A* **129**, 321 (1988); *Muon Catalyzed Fusion* **3**, 345 (1988).
- [9] P. Froelich, K. Szalewicz, H. J. Monkhorst, W. Kolos, and B. Jeziorski, in *Muon-Catalyzed Fusion*, edited by S. E. Jones, J. Rafelski, and H. J. Monkhorst, AIP Conf. Proc. No. 181 (AIP, New York, 1989), p. 259.
- [10] S. Hara and T. Ishihara, *Phys. Rev. A* **40**, 4232 (1989).
- [11] C. Y. Hu and A. K. Bhatia, *Phys. Rev. A* **43**, 1229 (1991).
- [12] P. Froelich, A. Flores-Riveros, and S. A. Alexander, *Phys. Rev. A* **46**, 2330 (1992).
- [13] P. Froelich and A. Flores-Riveros, *Phys. Rev. Lett.* **70**, 1595 (1993).
- [14] H. Feshbach, A. Kerman, and E. Lomon, *Ann. Phys. (N.Y.)* **41**, 1230 (1967).
- [15] G. Schulz, *Rev. Mod. Phys.* **45**, 378, 423 (1973).
- [16] I. Shimamura, *Phys. Rev. A* **40**, 4863 (1989).
- [17] S. A. Alexander, P. Froelich, and H. J. Monkhorst, *Phys. Rev. A* **41**, 2854 (1990); **43**, 2585(E) (1991).
- [18] L. N. Bogdanova, V. E. Markushin, V. S. Melezhik, and L. I. Ponomarev, *Yad. Fiz.* **34**, 1191 (1981) [*Sov. J. Nucl. Phys.* **34**, 662 (1981)].
- [19] L. N. Bogdanova, *Muon Catalyzed Fusion* **3**, 359 (1988).
- [20] L. Bracci, C. Chiccoli, G. Fiorentini, V. S. Melezhik, P. Pasini, L. I. Ponomarev, and J. Wozniak, *Muon Catalyzed Fusion* **4**, 247 (1989).
- [21] C. Chiccoli, V. I. Korobov, V. S. Melezhik, P. Pasini, L. I. Ponomarev, and J. Wozniak, *Muon Catalyzed Fusion* **7**,

- 87 (1992).
- [22] D. R. Bates, K. Ledsham, and A. L. Stewart, *Philos. Trans. R. Soc. London Ser. A* **246**, 215 (1953).
- [23] M. M. Madsen and J. M. Peek, *At. Data* **2**, 171 (1971); see also R. F. Wallis and H. M. Hulburt, *J. Chem. Phys.* **22**, 774 (1954).
- [24] M. C. Struensee, J. S. Cohen, and R. T. Pack, *Phys. Rev. A* **34**, 3605 (1986).
- [25] H. S. W. Massey and H. B. Gilbody, *Electronic and Ionic Impact Phenomena Vol. IV*, 2nd ed. (Oxford University Press, Oxford, 1974), pp. 2527 and 2528.
- [26] H. S. W. Massey and H. B. Gilbody, *Electronic and Ionic Impact Phenomena Vol. IV* (Ref. [25]), p. 2534, Eq. (340). [In Eq. (340) a factor of $1/4$ is missing, but this is corrected in Eq. (341a,b).]
- [27] R. G. Newton, *Scattering Theory of Waves and Particles* (McGraw-Hill, New York, 1966).
- [28] C. Y. Hu and A. K. Bhatia, in *Proceedings of the International Symposium on Muon Catalyzed Fusion, μ CF-89*, RAL Publ. No. RAL-90-022 (Rutherford Appleton Laboratory, Didcot, Oxfordshire, England, 1990), p. 73.
- [29] R. J. Oakes and C. N. Yang, *Phys. Rev. Lett.* **11**, 174 (1963).
- [30] J. Curiale and S. W. MacDowell, *Phys. Rev. D* **7**, 3461 (1973).
- [31] There are a number of differences between the results of Refs. [12] and [13], some small, some relatively large. The widths of the resonances have gotten smaller. Fusion rates have changed, too. See Table II. There are differences in the methods of calculation.
- [32] Comparisons can be made for expectation values of various quantities and the square of the Born-Oppenheimer wave function can be compared with the "pseudo-wave-function" squared (the three-body wave function squared, integrated over the muon's coordinates for fixed internuclear separation).
- [33] P. Froelich (private communication).
- [34] E. Borie and M. Leon, *Phys. Rev. A* **21**, 1460 (1981).
- [35] V. E. Markushin, *Zh. Eksp. Teor. Fiz.* **80**, 35 (1981) [*Sov. Phys.—JETP* **53**, 16 (1981)].
- [36] T. B. Day, G. A. Snow, and J. Sucher, *Phys. Rev. Lett.* **3**, 61 (1959).
- [37] J. S. Cohen and J. N. Bardsley, *Phys. Rev. A* **23**, 46 (1981).
- [38] The $\nu=8, J=0$ state of Ref. [10] at -1.6 eV has an outer classical turning point at $103a_\mu \approx 0.5a_0$. See Fig. 4 of Ref. [16].